

# Determination of Atmospheric Optical Properties During the First International Satellite Land Surface Climatology Project Field Experiment

Michael A. Spanner,\* Robert C. Wrigley,† and Rudolf F. Pueschel‡

*NASA Ames Research Center, Moffett Field, California 94035*

John M. Livingston‡

*SRI International, Menlo Park, California 94025*

and

David S. Colburn†

*NASA Ames Research Center, Moffett Field, California 94035*

Measurements of solar radiation were acquired with a multiwavelength, airborne, tracking sunphotometer during the First International Satellite Land Surface Climatology Project Field Experiment (FIFE). These measurements will permit the atmospheric correction of remotely sensed data acquired over the FIFE study area in eastern Kansas. Atmospheric optical properties derived from the sunphotometer measurements included total optical depth, aerosol optical depth, aerosol size distribution, aerosol phase function, and aerosol single scattering albedo. Data analyzed from two dates, June 6 and October 11, 1987, indicated the presence of aerosols with markedly different optical properties. Aerosol optical depths for the June 6 measurements exhibited a spectral dependence that peaked at the short wavelengths; whereas optical depths on October 11 decreased monotonically with wavelength and closely followed an Angstrom law wavelength dependence. Subsequent inversion of these data yielded a unimodal aerosol size distribution for June 6 and a power law size distribution (consistent with the Angstrom law wavelength dependence) for October 11. These differences are reflected in plots of the aerosol phase function. Variability of the atmospheric optical properties in both time and space illustrates the need to make sunphotometer measurements at the same time that remotely sensed data are acquired.

## Introduction

THE main objective of the International Satellite Land Surface Climatology Project (ISLSCP) is to derive quantitative information on land-surface climatological conditions from satellite observations of radiation reflected and emitted from the Earth. The First ISLSCP Field Experiment (FIFE) sponsored by NASA was conceived as a vehicle for the development and validation of methods to convert satellite-observed radiances into climatologically useful variables to analyze biosphere-atmosphere interactions. One set of problems associated with the quantitative use of satellite radiances to derive surface properties involves effects due to the intervening atmosphere. Not only does the atmosphere reduce the transmission of the incoming, reflected, and emitted radiation, but it contributes reflected and emitted radiation of its own. Under some conditions, atmospheric radiation comprises over 90% of the satellite-observed radiance, but even a much smaller effect would degrade the quantitative use of these data unless they are analyzed properly.

The interaction of radiation with the atmosphere is complex and has proved difficult to calculate without reference to measurements made at, or close to, the time and location of interest. Effects due to Rayleigh scattering from atmospheric

gases are well understood because the major gases (nitrogen and oxygen) that comprise 99% of the atmosphere are well mixed, and their concentrations with altitude are known; the small variations in surface pressure can be accounted for easily. The effects due to both small particle (aerosol) scattering and water vapor absorption are quite variable due to the wide range of aerosol and water vapor concentrations and to the variety of aerosols found in the atmosphere. Because aerosol and water vapor concentrations cannot be known a priori, they must be measured at the time and location of remote sensing data acquisition. Unfortunately, most remote sensing investigations have not been able to acquire this information. The FIFE Science Plan<sup>1</sup> specifically included acquisition of such data.

Many studies have shown that aerosols affect the transmission of electromagnetic radiation in the atmosphere. The sizes of the majority of aerosol particles are close to the wavelength of visible light.<sup>2</sup> The physical properties of aerosols such as size, shape, refractive index, and concentration in the atmosphere control the aerosol interaction with light according to a set of optical properties. Three fundamental properties are 1) the aerosol optical depth—an indirect measure of the size and number of particles present in a given column of air, 2) the single scattering albedo—the fraction of light intercepted that is scattered by a single particle, and 3) the phase function—a measure of the light scattered by a particle as a function of angle with respect to the direction of original propagation.

The goal of our research is to provide quantitative corrections for atmospheric effects in remotely sensed data acquired during FIFE. In this paper, we describe the use of an airborne tracking sunphotometer mounted on a NASA C-130 aircraft, which measured solar radiation at the same time as remotely sensed data were acquired. Aerosol optical depths were derived from the sunphotometer measurements by calculating

Presented as Paper 89-0818 at the AIAA 27th Aerospace Sciences Meeting, Reno, NV, Jan. 9-12, 1989; received March 3, 1989; revision received Sept. 8, 1989. Copyright © 1989 by the American Institute of Aeronautics and Astronautics, Inc. No copyright is asserted in the United States under Title 17, U.S. Code. The U.S. Government has a royalty-free license to exercise all rights under the copyright claimed herein for Governmental purposes. All other rights are reserved by the copyright owner.

\*Senior Research Scientist, TGS Technology, Inc.

†Research Scientist.

‡Senior Research Meteorologist.

the total atmospheric optical depths and then subtracting the best estimates of optical depths due to Rayleigh scattering, ozone, and nitrogen dioxide. The aerosol optical depths were subsequently inverted to yield estimates of the columnar aerosol size distributions, from which corresponding phase functions and single scattering albedos were calculated using Mie theory. These data will be used in radiative transfer models to remove atmospheric effects from remotely sensed data acquired during FIFE.

## Background

### Airborne Tracking Sunphotometer

Sunphotometry has been a successful technique for measuring multiwavelength aerosol optical depths for some time. Historically, nearly all measurements have been ground based.<sup>3-6</sup> One problem with ground-based measurements is that they do not yield information on the vertical profile of optical depth. To obtain information necessary to correct aircraft acquired remotely sensed data for atmospheric effects requires information on the optical properties of the atmosphere between the ground and the sensor. Acquisition of optical information on the vertical profile is only possible using an airborne sunphotometer. A second disadvantage with ground-based sunphotometry is that regional variations of optical depths cannot be characterized unless sunphotometer networks are established. Airborne sunphotometry, on the other hand, provides optical depth information at a spatial scale required by FIFE with only one instrument.

The airborne tracking sunphotometer is mounted outside the C-130 aircraft cabin and automatically tracks the sun. The detector module contains six separate silicon photodetectors, which view the sun simultaneously at six independent wavelengths with a two degree field of view.<sup>7,8</sup> Table 1 shows the wavelengths and the full-width half maximum (FWHM) for the detector module used during FIFE. The present data acquisition rate is 0.5 Hz corresponding to a spatial sampling resolution of 200 m at an aircraft speed of 100 m s<sup>-1</sup>. The solar tracking system automatically locates the sun if it is within 25 deg and tracks it to an accuracy of better than 0.2 deg. The large field of view of the sun tracker simplifies initial pointing and allows reacquisition of the sun if tracking is lost due to abrupt aircraft movements or interception of an optically thick cloud.

### First ISLSCP Field Experiment

During the late spring, summer and fall of 1987, FIFE conducted its major field efforts at the Konza Prairie, Kansas, and surrounding grassland areas during four Intensive Field Campaigns (IFC) of approximately two weeks each.<sup>9</sup> The C-130 flew with the airborne tracking sunphotometer and a suite of remote sensing instruments including the NS001 Thematic Mapper Simulator, the Thermal Infrared Multispectral Scanner, the Push Broom Microwave Radiometer, and the Advanced Solid State Array Sensor. Additionally, remote sensing data were acquired from several Earth-orbiting satellites including the Advanced Very High Resolution Radiometer (AVHRR) on two National Oceanic and Atmospheric Administration satellites NOAA-9 and NOAA-10, the Geostationary Orbiting Environmental Satellite (GOES), the Systeme Probatoire d'Observation de la Terre (SPOT), and Landsat.

Table 1 Detector wavelength set for FIFE

Wavelength, nm	Full-width half maximum, nm
380	12.1
450	5.5
526	12.1
600	10.3
940	14.4
1020	12.1

In addition to radiance measurements made by ground and helicopter-mounted spectral radiometers, intensive measurements of meteorological conditions, soil moisture, heat, water vapor, and radiation fluxes were made. Several aircraft measured momentum, heat, moisture, and carbon dioxide fluxes over the Konza Prairie to monitor the atmospheric boundary layer. These data are being shared by over 30 FIFE investigators to analyze biosphere-atmosphere interactions in support of the goals and objectives of ISLSCP.

### Atmospheric Correction Approach

Although still in its formative stages, our approach to the atmospheric correction of remotely sensed data for FIFE will take three steps. First, it will be necessary to make sure all the radiometric and atmospheric measurements form a complete and consistent description of the system. This involves radiation entering the top of the atmosphere, its interaction with the atmosphere, reflection from the surface back into the atmosphere, and finally, its measurement by a remote sensing instrument. Unless all the terms balance, the atmospheric correction problem will not be solvable: at least one of the measurements will be lacking or faulty. If a complete, well-understood, but one-dimensional model of the atmosphere/surface/sensor system is used for this step, the fault will probably lie in the calibration of the surface or remote sensing radiometers. Given the most accepted values for extraterrestrial irradiances<sup>10</sup> and optical depths for Rayleigh scattering,<sup>11,12</sup> it may be necessary to adjust the calibration of these radiometers to achieve a consistent description. A variant of this approach permitted analysis of Coastal Zone Color Scanner data to achieve a consistent calibration of the instrument within 1% and implementation of reasonably accurate atmospheric correction procedures.

The second step in our approach to atmospheric correction is to formulate a simpler atmospheric model using a single scattering approximation, which permits the separation of Rayleigh scattering from scattering caused by aerosols. A somewhat more complex version of this approach would allow multiple Rayleigh scattering while keeping the aerosol scattering separate. The simplified model of the radiances,  $L$ , at each wavelength, received at the sensor can be written

$$L_t = L_p + T_p L_s \quad (1)$$

where the subscripts  $t$ ,  $p$ , and  $s$  refer to quantities at the sensor, atmosphere, and surface, respectively, and  $T$  is the diffuse transmittance. The surface radiance  $L_s$  is the quantity we must solve for. The transmittance can be written

$$T_p = \exp[-\tau(1/\mu + 1/\mu_0)] \quad (2)$$

where the total optical depth  $\tau$  is the sum of optical depths due to Rayleigh and aerosol scattering, water vapor, ozone, and nitrogen dioxide absorption,  $\mu$  is the cosine of the zenith angle to the sensor, and  $\mu_0$  is the cosine of the solar zenith angle. The path radiance can be decomposed according to the single scattering approximation:

$$L_p = L_r + L_a \quad (3)$$

where  $r$  and  $a$  refer to the Rayleigh and aerosol components. Both of these path radiances can be written as

$$L_x = \omega_x \tau_x F_0 T_{03} / 4\pi\mu \quad (4)$$

Hence, in addition to the Rayleigh and aerosol optical depths  $\tau_x$ , it will be necessary to estimate the single scattering albedos  $\omega_x$  and the scattering phase functions  $P_x$ . The Rayleigh phase function is well known, and  $\omega_r = 1$ . King et al.<sup>13</sup> presented a method for deriving an aerosol size distribution from multiwavelength aerosol optical depth measurements. The aerosol size distribution can be used in Mie theory cou-

pled with reasonable assumptions about the index of refraction of the aerosols to estimate the aerosol single scattering albedo and the aerosol phase function. The other variables in the equation are more tractable. The extraterrestrial irradiances  $F_0$  in each spectral band of the remote sensing instrument are determined by convolving the spectral response of the band with the measurements of Neckel and Labs.<sup>10</sup> The ozone transmittances  $T_{O_3}$ , use ozone concentrations modeled by van Heuklon<sup>14</sup> for the full atmospheric path. With the determination of these parameters, the single scattering model is complete and will permit the derivation of the surface radiances.

The third step in our atmospheric correction approach is to extend the single scattering model. One possibility has been mentioned previously: incorporate multiple Rayleigh scattering while still treating aerosol scattering separately. Another possibility is to modify a two-stream radiative flux model to obtain directional values or radiances.

## Methods

### Data Collection

Sunphotometer data were collected during all of the daytime flights of the C-130 during the four IFCs. Data were acquired concurrently with the NS001 Thematic Mapper Simulator and the other instruments at approximately 1850, 3350, and 5200 m altitude mean sea level (msl) for flight lines over the Konza Prairie. Data were acquired simultaneously with SPOT, Landsat, and NOAA-9 and NOAA-10 overpasses on numerous occasions. During ascent and descent of the C-130 sunphotometer, data were collected, providing altitudinal profiles of optical depth. Sunphotometer measurements were made before and after flights at the Manhattan, Kansas, airport to allow measurement of the entire atmospheric slab. During the ferry run between California and Kansas on October 4, 1987, measurements were acquired that permitted a calibration of the sunphotometer.

### Data Analysis

Measurements of solar radiation were obtained in the form of voltage from the six photodetectors of the sunphotometer. Each voltage was assumed to be proportional to the directly transmitted solar irradiance averaged over the corresponding filter spectral bandwidth intercepted by the detector. For all sunphotometer channels except 940 nm, it was assumed that the attenuation of solar radiation was adequately described by the Bouguer-Lambert-Beer extinction law:

$$V = (R'/R)^2 V_0 e^{-m\tau} = V'_0 e^{-m\tau} \quad (5)$$

where  $V$  is the output voltage of the detector at a given wavelength,  $V_0$  is the zero air-mass voltage intercept at that wavelength for the mean Earth-sun separation  $R'$ ,  $R$  is the Earth-sun separation at the time of observation,  $m$  is the atmospheric air mass between the instrument and the sun,  $\tau$  is the wavelength-dependent total vertical optical depth above the sunphotometer, and  $V'_0$  is the zero-air-mass voltage intercept for the Earth-sun separation  $R$  at the time of observation. This assumption is valid if the amount of diffusely scattered light collected by the sunphotometer is negligible, a condition that is generally satisfied for measurements under background (cloud-free and smoke-free) atmospheric conditions. Characterization of the attenuation in the 940 nm channel is complicated by water vapor absorption bands that, in general, do not follow Beer's law.

### Calibration

To derive reliable estimates of spectral optical depth from multiwavelength sunphotometer measurements, precise values of the intercept voltages must be used in Eq. (5). These values are estimates of the voltages that the instrument would measure if it were positioned at the top of the atmosphere. The

intercept voltages were derived using the NASA Langley plot calibration method. The least-squares regression line fitting the logarithm of  $V$  plotted against air-mass  $m$  was calculated, thus obtaining  $V'_0$  by extrapolation to zero air mass:

$$\ln V = \ln V'_0 - m\tau \quad (6)$$

The intercepts change over time due to filter degradation, drift in amplifier gain, detector alignment, or variation in the solar constant. For the FIFE data acquisition period, intercept voltages were calculated by interpolation using values derived from airborne measurements obtained on March 12 and October 4, 1987, and ground-based measurements obtained at Mauna Loa Observatory, Hawaii, during a six-day period in early spring 1988.

### Derivation of Aerosol Optical Depths

Measurements obtained during FIFE were screened to remove low detector voltages due to attenuation by clouds, loss of sun acquisition during steeply banked turns, or obstruction of the sun by the C-130 tail section. Air mass was calculated as a function of time from solar ephemeris data. Corresponding total spectral optical depths were calculated using Eq. (5). The total optical depths included attenuation due to molecular scattering, aerosol extinction, and gaseous absorption:

$$\tau_t = \tau_r + \tau_a + \tau_{O_3} + \tau_{NO_2} + \tau_{H_2O} \quad (7)$$

where the primary gaseous absorbers are nitrogen dioxide (primarily in the 380- and 450-nm bands), ozone (in the 526- and 600-nm channels), and water vapor (in the 940-nm band). Aerosol optical depths were calculated from Eq. (7) after making reasonable estimates of the Rayleigh and gaseous optical depth contributions. Rayleigh optical depths were calculated from the aircraft altimeter measurements and a model atmosphere. Optical depths due to absorption by nitrogen dioxide were interpolated from stratospheric column content measurements by Noxon<sup>15</sup> and were less than 0.01 at all wavelengths. It was assumed that absorption by tropospheric nitro-

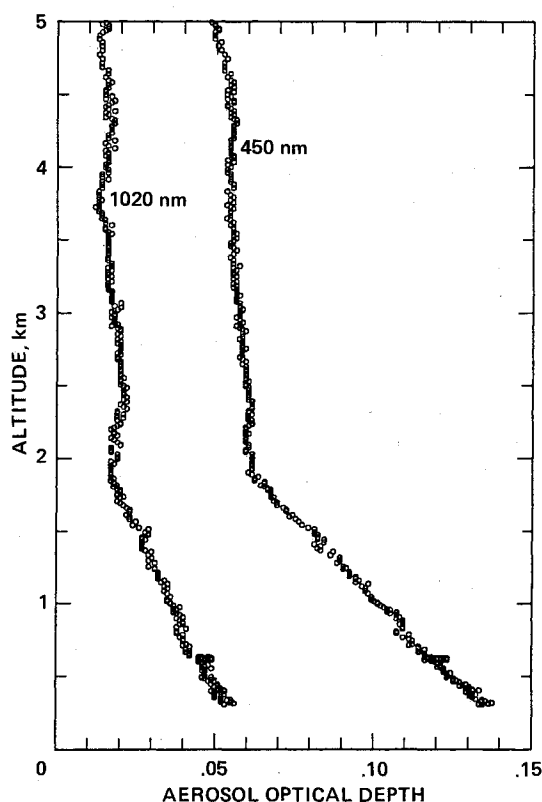


Fig. 1 Vertical profile of aerosol optical depth acquired during spiral descent over the FIFE study area on June 6, 1987.

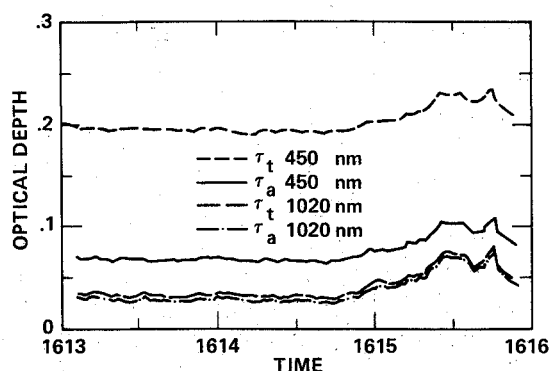


Fig. 2 Variation of total and aerosol optical depths at 450 and 1020 nm along a 5-km flight line (expressed as a function of time) at an altitude of 4900 m msl on June 6, 1987, for 450 nm,  $\tau_{\text{NO}_2} = 0.0076$  and  $\tau_{\text{O}_3} = 0.0010$ .

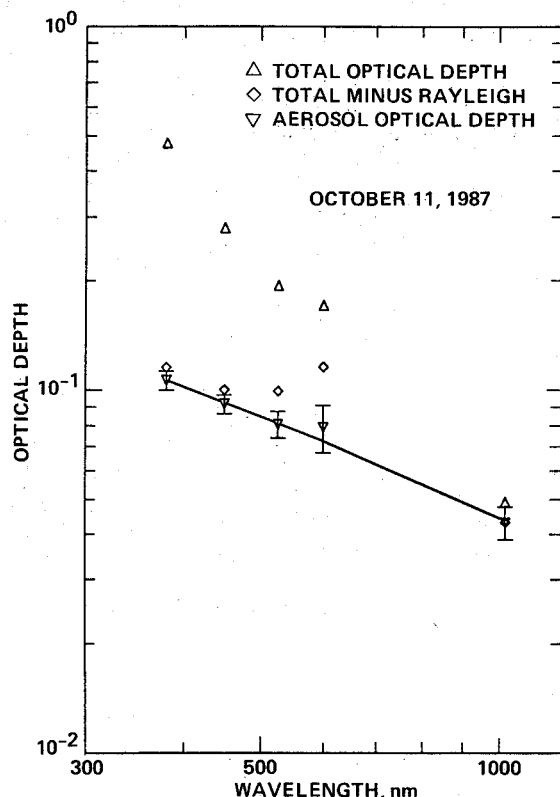


Fig. 3 Mean spectral optical depths derived from measurements made on October 11, 1987; error bars depict  $\pm 1\sigma$  and uncertainties in the observed aerosol optical depths; the curve indicates the regression fit to the data using the inverted aerosol size distribution.

gen dioxide was negligible. Estimates of ozone optical depths were determined from the climatological stratospheric ozone column content model of van Heuklon,<sup>14</sup> which yielded optical depth values of about 0.032 at 600 nm and 0.014 at 526 nm for the Konza Prairie based on an ozone column content of 290 matm cm. A more complete description of optical depth corrections applied to measurements obtained with the airborne sunphotometer is presented in Pueschel et al.<sup>16</sup>

### Results

Airborne tracking sunphotometer data acquired during FIFE were reduced to optical depths and submitted to the FIFE information system for use by all FIFE investigators for "golden and silver days," those days when conditions permitted most of the important measurements to be made. Optical depths were reported every 2 s for individual flight lines, ascents, descents, satellite overpasses, and surface measure-

ments before and after flights. For each listing, the following quantities were provided: time, latitude, longitude, altitude, total optical depths for the six wavelengths, net optical depths (total optical depth minus the Rayleigh optical depth) for 380, 450, 526, 600, and 1020 nm, and the water vapor overburden derived from the 940-nm channel. A header file for each group of measurements was provided that contained ancillary information on the zero air-mass voltages used, ozone optical depths and nitrogen dioxide optical depths. In the following sections, examples of data are presented as well as products derived from them including plots of spectral optical depths, aerosol size distributions, aerosol phase functions, and aerosol single scattering albedos. In these examples, ozone and nitrogen dioxide optical depths have been subtracted from the net optical depths.

### Optical Depths

Figure 1 presents vertical profiles of aerosol optical depths at 450 and 1020 nm during a descent of the C-130 on June 6, 1987. The atmospheric boundary layer is well defined by the profile and extends from the surface to approximately 2 km. This conforms to measurements of the atmospheric boundary layer made by other FIFE investigators using flux measurements aboard aircraft.

Figure 2 shows optical depths derived from measurements obtained on June 6, 1987 at approximately 4900 m msl. Three min of data (representing approximately 90 sunphotometer observations) are shown for total and aerosol optical depths at 450 and 1020 nm. At 450 nm most of the total optical depth is due to Rayleigh scattering with a very minor contribution from nitrogen dioxide absorption. The remainder, the aerosol optical depth, shows a 50% variation along this short (5 km) flight line. At 1020 nm, most of the total optical depth is due to the aerosols with only a small Rayleigh contribution. Not only does the variation in aerosol optical depth along the flight line exceed 100%, but its correspondence to the aerosol optical depth at 450 nm is remarkable and extends to some of the smaller variations along the flight line. There were no clouds

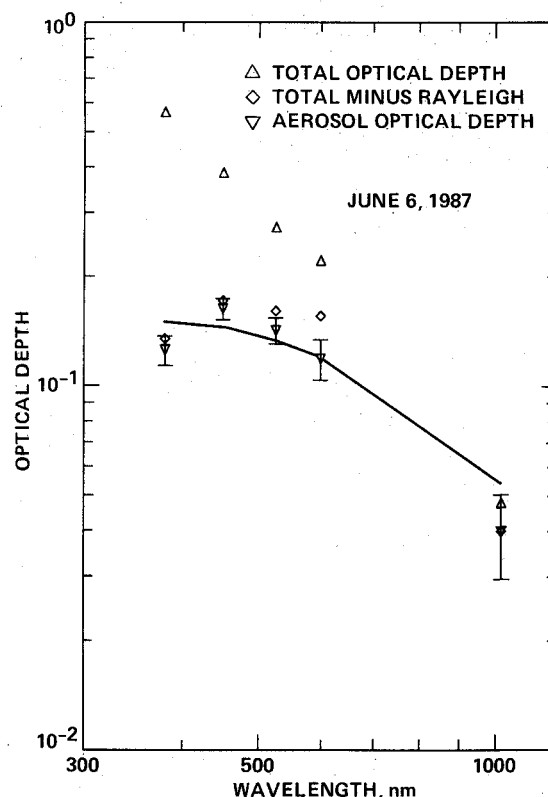


Fig. 4 Mean spectral optical depths derived from measurements made on June 6, 1987.

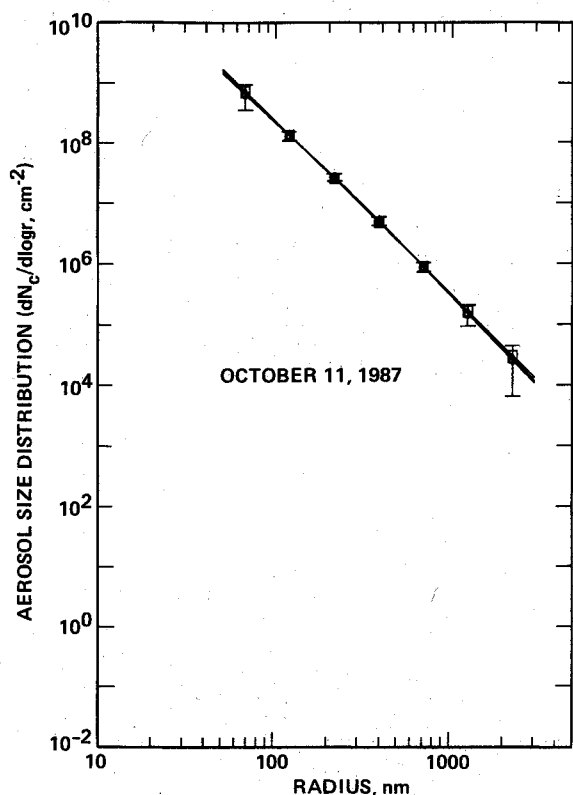


Fig. 5 Estimated columnar aerosol size distribution and associated uncertainties derived from the inversion of spectral optical depth data (October 11, 1987) shown in Fig. 3.

or haze observed at the time of data acquisition according to the all-sky cameras.<sup>17</sup> This result calls into question the often assumed constancy of aerosol optical depths over such short distances.

No other determinations of aerosol optical depths were available for intercomparison on either June 6 or October 11, 1987. Two ground-based sunphotometers made measurements of optical depths nearly simultaneously with ground measurements by the airborne tracking sunphotometer on July 10–11, 1987. Intercomparisons of aerosol optical depths calculated using a sunphotometer from NASA Goddard Space Flight Center showed good agreement, in general, with differences of 0.02 to 0.08 units of optical depth.<sup>18</sup> Similar comparisons performed with a sunphotometer from the Jet Propulsion Laboratory (JPL) indicated that the JPL instrument was consistently lower by approximately 0.05 units of optical depth. These differences are considered to be acceptable.

#### Spectral Dependence of Aerosol Optical Depths

The spectral dependence of aerosol optical depth is often described according to Angstrom<sup>19</sup>:

$$\tau\lambda = \tau\lambda_1(\lambda/\lambda_1)^{-n} \quad (8)$$

where  $\lambda_1$  is a reference wavelength, and  $n$  is the Angstrom exponent, which is usually in the range of 1–2 for background aerosols. Figure 3 shows the spectral dependence of optical depth on October 11, 1987, for a 1800-m msl flight line that exhibited very little variation in optical depth. The solid curve indicates the regression fit to the data from the inverted aerosol size distribution using the technique of King et al.<sup>13</sup>; this line connects aerosol optical depths that have been calculated from the inverted size distribution. It is virtually indistinguishable from an Angstrom law dependence with an exponent of  $0.90 \pm 0.08$ . The aerosol optical depth at 600 nm is slightly elevated from the regression fit. This may indicate insufficient

compensation for ozone or instrumental anomalies with the 600-nm detector, which had been observed from time to time.

Figure 4 shows the spectral dependence for the optical depths at the surface on June 6, 1987, a few hours prior to acquisition of the data shown in Fig. 2. Almost all the corresponding optical depths are somewhat higher than in both Figs. 2 and 3, as might be expected for a surface location. The spectral dependence of the aerosol optical depths can no longer be characterized by the straight-line relationship of the Angstrom law. The aerosol optical depth at 380 nm is significantly lower than at 450 nm, suggesting that the aerosol size distribution falls off at low radii. Several possibilities for errors in data processing were examined to explain this result but none were found that would eliminate the effect. Similar results were also observed in other data from this date (both the high and low optical depth regions of the flight line at 4900 m shown in Fig. 2). The aerosol optical depth at 380 nm was lower than at 450 nm in both instances. We concluded that this result was characteristic for the atmosphere on that date. Note that the 600-nm aerosol optical depth appears to be consistent with surrounding values.

Subtracting the spectral optical depths of the low optical depth region of the data presented in Fig. 2 from those of the high optical depth region resulted in differences that were optically neutral ( $n = 0$ ). This type of spectral dependence is typical of cirrus clouds lending credence to the existence of subvisible cirrus clouds above 5000 m.

#### Inversion to Obtain Aerosol Size Distributions

The aerosol optical depths shown in Fig. 3 for October 11, 1987, were inverted to estimate columnar aerosol size distributions. The size distributions shown in Fig. 5 are results from the first, fourth, and final (eighth) iterations of the constrained linear inversion procedure. The results of the iterations are nearly indistinguishable in Fig. 5 and closely approximate a power law distribution. This result is not surprising since the initial size distribution was a power law relationship

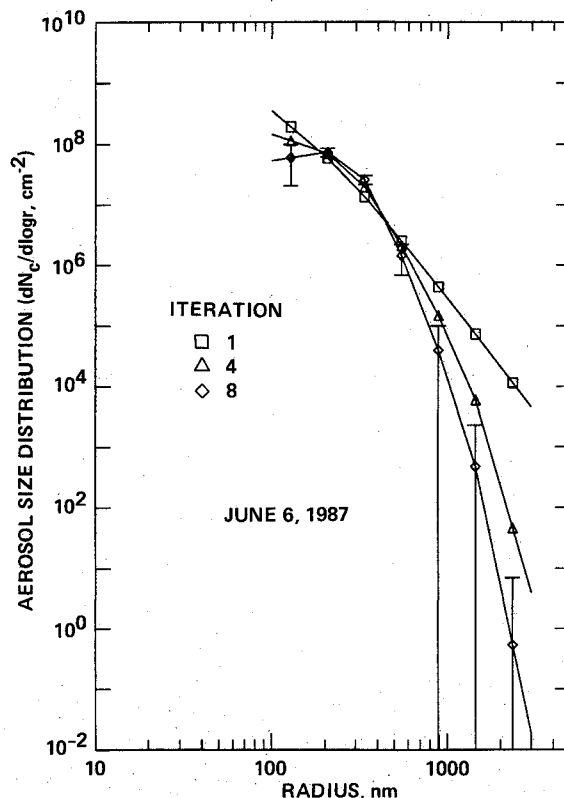


Fig. 6 Estimated columnar size distribution and associated uncertainties derived from the inversion of spectral aerosol optical depth data (June 6, 1987) shown in Fig. 4.

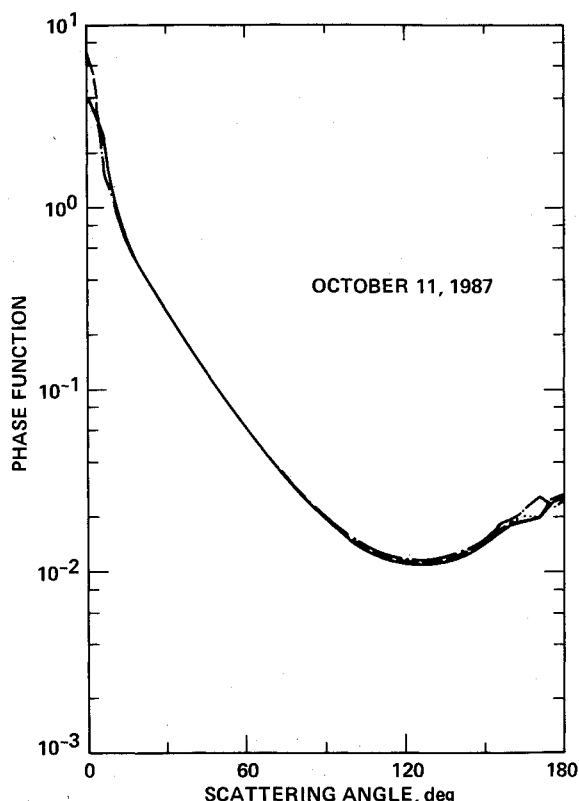


Fig. 7 Phase function calculated from aerosol size distribution for data obtained on October 11, 1987.

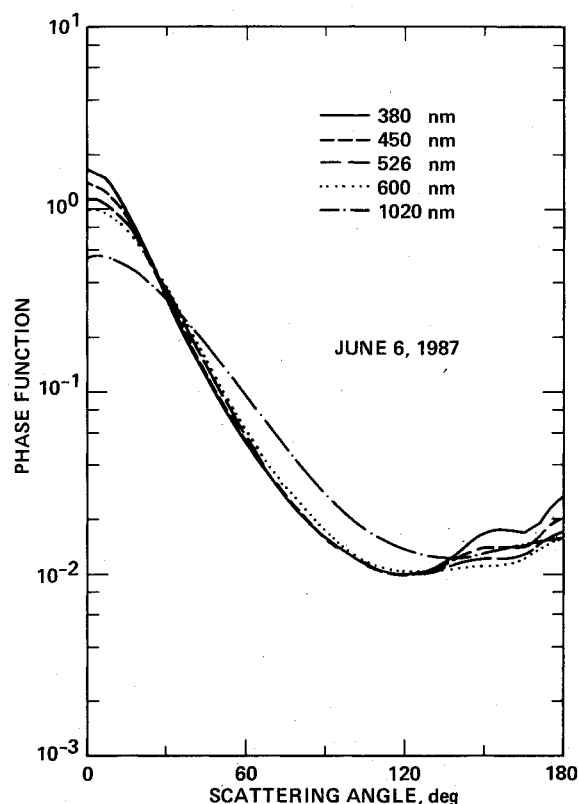


Fig. 8 Phase function calculated from aerosol size distribution for data obtained on June 6, 1987.

that was calculated by assuming an Angstrom law dependence. The inversion was carried out over the radius range of 50 to 3000 nm with an index of refraction of  $1.50-0.01i$ , which is reasonable for Kansas. King et al.<sup>13</sup> showed that inversion is not very sensitive to the exact choice of the index of refraction. The columnar aerosol size distribution was used to obtain a regression fit to the aerosol optical depths, and the result is shown as the solid curve through the aerosol optical depths in Fig. 3. The regression provides an excellent fit to the data.

Figure 6 displays the results of the inversion process for the spectral-aerosol optical depth data shown in Fig. 4 for June 6, 1987. The size distributions for the first, fourth, and final iterations are shown. The final iteration shows a peak in the columnar distribution at 200 nm in radius. The peak is a direct consequence of the decrease in aerosol optical depth from 450 to 380 nm. The changes in the columnar size distributions throughout the iterations indicates the degree of difficulty the procedure had in satisfying the constraints on the inversion process. This is also observed by the regression fit the size distribution yielded for the spectral optical depths as shown by the solid curve in Fig. 4. The curve does not pass through the specified error limits.

#### Aerosol Phase Function and Single Scattering Albedo

Figures 7 and 8 show the normalized phase functions calculated from the inverted aerosol size distributions for data obtained on October 11 and June 6, 1987, respectively. The phase functions are normalized to yield a total scattering probability of unity. As expected, the phase functions are peaked predominantly in the forward direction and, to a lesser extent, in the backward direction. There is more forward scattering observed in the plot of the October 11 data than is observed in the June 6 data. This is a result of the differences in the two aerosol size distributions since the other parameters were held constant. Additionally, there is a distinct wavelength dependence to the phase functions calculated from the June 6 data that is not observed in the October 11 data. The

single scattering albedo calculated for sunphotometer data acquired on October 11 ranged from 0.889 to 0.891, whereas for June 6 it ranged from 0.935 to 0.950. These results are a function of the assumed refractive index of  $1.5-0.01i$ .

#### Summary

Because the objective of FIFE is to derive quantitative information on land surface climatological conditions from satellite remote sensing measurements, it is necessary to quantify the effect of the atmosphere on these data. From measurements of solar radiation made by the airborne tracking sunphotometer, atmospheric optical properties necessary to perform atmospheric corrections were calculated. Variability in atmospheric optical properties across some of the flight lines illustrates the need for an instrument that can measure this spatial variation. Substantial differences in atmospheric optical properties were observed in the June 6 and October 11 data sets. These differences emphasize the need to make quantitative measurements of atmospheric optical properties at the time of remote sensing data acquisition. The atmospheric optical properties calculated from measurements made by the airborne tracking sunphotometer will allow atmospheric corrections to be performed to the remotely sensed data acquired during FIFE.

#### Acknowledgments

This research was supported by the Land Processes Branch of the NASA Earth Science and Applications Division. The authors gratefully acknowledge Duane Allen of NASA Ames Research Center for operation and maintenance of the airborne tracking sunphotometer.

#### References

- <sup>1</sup>Schmugge, T., and Sellers, P., "FIFE Science Plan," *Experiment Plan for the First ISLSCP Field Experiment (FIFE)*, NASA Goddard Space Flight Center, Greenbelt, MD, 1986.

<sup>2</sup>Whitby, K., "The Physical Characteristics of Sulfur Aerosols," *Atmospheric Environment*, Vol. 12, 1978, pp. 135-159.

<sup>3</sup>Flowers, C., McCormick, R., and Kurfis, K., "Atmospheric Turbidity Over the United States, 1961-1966," *Journal of Applied Meteorology*, Vol. 8, 1969, pp. 955-962.

<sup>4</sup>Shaw, G., Reagan, J., and Herman B., "Investigations of Atmospheric Extinction Using Direct Solar Radiation Measurements Made with a Multiple Wavelength Radiometer," *Journal of Applied Meteorology*, Vol. 12, 1973, pp. 374-380.

<sup>5</sup>Russell, P., Scribner, E., and Uthe, E., "An Automated Multi-wavelength Sunphotometer to Characterize Transient Aerosol and Water Vapor Events," *Third Conference on Atmospheric Radiation*, American Meteorological Society, Boston, MA, 1979.

<sup>6</sup>Bird, R., and Hulstrom, R., "Precipitable Water Measurements with Sunphotometers," *Journal of Applied Meteorology*, Vol. 21, 1982, pp. 1196-1201.

<sup>7</sup>Russell, P., Matsumoto, T., Banta, V., Livingston, J., Mina, C., Colburn, D., and Pueschel, R., "Measurements With an Airborne, Autotracking, External-Head Sunphotometer," *Proceedings of the Sixth Conference on Atmospheric Radiation*, American Meteorological Society, Boston, MA, May 1986.

<sup>8</sup>Matsumoto, T., Russell, P., Mina, C., Van Ark, W., and Banta, V., "Airborne Tracking Sunphotometer," *Journal of Atmospheric and Oceanic Technology*, Vol. 4, No. 2, 1987, pp. 336-339.

<sup>9</sup>Sellers, P., Hall, F., Asrar, G., Strebel, D., and Murphy, R., "The First ISLSCP Field Experiment (FIFE)," *Bulletin American Meteorological Society*, Vol. 69, No. 1, 1988, pp. 22-27.

<sup>10</sup>Neckel, H., and Labs, D., "The Solar Radiation Between 3300

and 12500 Å," *Solar Physics*, Vol. 77, 1984, pp. 205-258.

<sup>11</sup>Frohlich, C., and Shaw, G., "New Determination of Rayleigh in the Terrestrial Atmosphere," *Applied Optics*, Vol. 19, 1980, pp. 1773-1775.

<sup>12</sup>Young, A., "Revised Polarization Corrections for Atmospheric Extinction," *Applied Optics*, Vol. 22, 1980, pp. 3427-3428.

<sup>13</sup>King, M., Bryne, D., Herman, B., and Reagan, J., "Aerosol Size Distributions Obtained by Inversion of Spectral Optical Depth Measurements," *Journal of Atmospheric Sciences*, Vol. 35, 1978, pp. 2153-2167.

<sup>14</sup>Van Heuklon, T., "Estimating Atmospheric Ozone for Solar Radiation Models," *Solar Energy*, Vol. 22, 1979, pp. 63-68.

<sup>15</sup>Noxon, J., "Stratospheric NO<sub>2</sub>, 2, Global Behavior," *Journal of Geophysical Research*, Vol. 84, 1979, pp. 5067-5076.

<sup>16</sup>Pueschel, R., Livingston, J., Russell, P., Colburn, D., Ackerman, T., Allen, D., Zak, B., and Einfeld, W., "Smoke Optical Depths: Magnitude, Variability and Wavelength Dependence," *Journal of Geophysical Research*, Vol. 93, 1988, pp. 8388-8402.

<sup>17</sup>Henderson-Sellers, A., private communication, 1988.

<sup>18</sup>Wrigley, R., and Spanner, M., "Comparison of Aerosol Optical Depth Measured by Three Groups During FIFE," *EOS*, Vol. 70, 1989, p. 344.

<sup>19</sup>Angstrom, T., "On the Atmospheric Transmission of Sun Radiation and on Dust in the Air," *Geogr. Ann.*, Vol. 11, 1929, pp. 156-166.

Henry B. Garrett  
Associate Editor

*Recommended Reading from the AIAA  
Progress in Astronautics and Aeronautics Series . . .*



## **Monitoring Earth's Ocean, Land and Atmosphere from Space: Sensors, Systems, and Applications**

*Abraham Schnapf, editor*

This comprehensive survey presents previously unpublished material on past, present, and future remote-sensing projects throughout the world. Chapters examine technical and other aspects of seminal satellite projects, such as Tiros/NOAA, NIMBUS, DMS, LANDSAT, Seasat, TOPEX, and GEOSAT, and remote-sensing programs from other countries. The book offers analysis of future NOAA requirements, spaceborne active laser sensors, and multidisciplinary Earth observation from space platforms.

**TO ORDER: Write, Phone, or FAX: AIAA c/o TASC0,**  
9 Jay Gould Ct., P.O. Box 753, Waldorf, MD 20604  
Phone (301) 645-5643, Dept. 415 ■ FAX (301) 843-0159

Sales Tax: CA residents, 7%; DC, 6%. For shipping and handling add \$4.75 for 1-4 books (call for rates for higher quantities). Orders under \$50.00 must be prepaid. Foreign orders must be prepaid. Please allow 4 weeks for delivery. Prices are subject to change without notice. Returns will be accepted within 15 days.

**1985 830 pp., illus. Hardback**  
**ISBN 0-915928-98-1**  
**AIAA Members \$59.95**  
**Nonmembers \$99.95**  
**Order Number V-97**